A COMPARATIVE STUDY OF DIFFERENT CHIP SEPARATION APPROACHES FOR NUMERICAL MODELING OF ORTHOGONAL CUTTING

Bo Hou[1], Yong-fu Wu[1], Shu-hui Li[1,2], Zhong-qin Lin[1,2] and Zhong-qi Yu[1,2]
[1]*Shanghai Key Laboratory of Digital Autobody Engineering, Shanghai Jiao Tong University*
800 Dongchuan RD., Shanghai, China
[2]*State Key Laboratory of Mechanical System and Vibration, Shanghai, China*

Keywords: Dry cutting, Modelling, ALE, Damage evolution, Residual stress.

Abstract: Numerical cutting modelling gives access to thermo-mechanical field such as stress, strain and temperature that are difficult to obtain through experiments, thus provides a unique insight and helps to improve design quality and shorten design cycle. Chip separation is one of the most important issues in cutting simulation because of its significant influence on chip formation, stress and temperature predictions. Modelling of an orthogonal cutting process using ABAQUS/explicit is presented. Two kinds of chip separation approaches are compared, a partial damage zone (PDZ) and an Arbitrary-Lagrangian-Eulerian (ALE) based approach, with the aim to characterize the effect on chip formation, cutting force, temperature and residual stress. ALE and PDZ methods predict the similar cutting force and temperature results, and they also predict different chip formations and residual stress profiles. The predictions are analysed and possible reasons are discussed.

1 INTRODUCTION

Numerical cutting modelling are more and more essential in predicting chip formation, cutting forces, distributions of strain, strain rate, stress, and cutting temperature. Therefore, it provides a unique insight for fundamental understanding of the machining process, which leads to proper choice or design of cutting tools, fixture, spindle, feed, and reduction of lengthy and costly design iterations experimentation required for process optimization.

Reliable cutting simulation heavily depends on the chip separation approaches, which are based on three main formulations. The first one is the Lagrangian formulation, in which the elements are attached to the material. Shet and Deng (2003:573-583) applied Lagrangian model for orthogonal cutting simulation, in which the chip separation was modelled by nodal release based on critical stress criterion. In the study of Hortig and Svendsen (2007:66-76), the continuous chip was formed along a predefined separation path based on the fracture criterion and element deletion. Ng et al (2002:301-329) and Mabrouki et al (2008:1187-1197) studied saw-tooth chip formation with a predefined separation path, as well as a damage law for modelling fragmented chip behaviour. The chip separation approaches based on Lagrangian formulation are generally base on partial damage zone (PDZ) corresponding to the trajectory of the tool-tip. However, the PDZ must be predefined which is difficult for 3D milling modelling. Furthermore, the global damage zone (GDZ) approach is applied for chip separation, in which each element is assessed for damage over the mesh and all time increments. Pantalé et al (2004:4383-4399) and Anurag et al (2009:303-317) studied orthogonal and 3D milling process using GDZ approach with no pre-defined sacrificial element or zipped nodes to be split.

The Eulerian formulation, in which the element is not attached to the material, handles material flow around tool tip without the need to define a failure criterion (Nasr, Ng and Elbestawi, 2007:401-411). However, the chip shape has to be known a priori, which represents a huge drawback. Furthermore, residual stress cannot be estimated because the material elastic behaviour is not considered (Movahhedy, Gadala and Altintas, 2000:267-275). Studies using Eulerian formulation for chip separation are reported by Kim et al (1999:45-55)

Hou B., Wu Y., Li S., Lin Z. and Yu Z..
A COMPARATIVE STUDY OF DIFFERENT CHIP SEPARATION APPROACHES FOR NUMERICAL MODELING OF ORTHOGONAL CUTTING.
DOI: 10.5220/0003646004580464
In *Proceedings of 1st International Conference on Simulation and Modeling Methodologies, Technologies and Applications* (SDDOM-2011), pages 458-464
ISBN: 978-989-8425-78-2

and Strenkowski et al (2002:723-731).

The Arbitrary-Lagrangian-Eulerian (ALE) formulation combines the features of Lagrangian and Eulerian analysis. The Eulerian technique is perfect for modelling the material flow around tool tip, while the Lagrangian technique is suitable for modelling the unconstrained material flow at the free boundaries. Therefore, the thermo-mechanical field surrounding the tool tip can be analysed more reliably, together with the absence of separation criterion, which is always necessary in Lagrangian model. As a result, the residual stress can be calculated with enough accuracy which is impossible in Eulerian models (Nasr, Ng and Elbestawi, 2008:149-161). However, serrated chip cannot be modelled with this technique. Another drawback is the necessity to precisely define the previous geometry of the chip.

Different chip separation approaches are adopted in cutting simulations for different purposes, such as prediction of chip formation, cutting force and residual stress. However, a systematic comparison of them has not been reported yet. It is difficult to estimate the practical effects of different approaches for the same material and cutting process. This paper aims to estimate PDZ and ALE based chip separation approaches in terms of chip formation, stress, temperature distribution and cutting force prediction during orthogonal cutting of an aeronautic aluminium alloy Al7050-T7451, which is generally used as the structural material of aircraft.

2 NUMERICAL MODEL

2.1 Material Constitutive Model

The Johnson-Cook material model is utilized. Assuming a von Mises type yield criterion and an isotropic strain hardening rule, the flow stress is given by

$$\sigma = \left(A + B\bar{\varepsilon}^{n}\right)\left(1 + C\ln\frac{\dot{\bar{\varepsilon}}}{\dot{\bar{\varepsilon}}_0}\right)\left[1 - \left(\frac{T - T_0}{T_{\text{melt}} - T_0}\right)^{m}\right] \qquad (1)$$

where $\bar{\varepsilon}$ is the equivalent plastic strain. $\dot{\bar{\varepsilon}}$ and $\dot{\bar{\varepsilon}}_0$ are the equivalent plastic strain rate and a reference strain rate, respectively. T, T_0 and T_{melt} stand for temperature, reference temperature and melting temperature, respectively. A, B, C, m and n are material parameters.

There are two popular experimental methods to obtain the flow stress data under cutting condition: Split Hopkinson pressure bar (SHPB) (Lennon and Ramesh, 1998:1279-1292) and Orthogonal cutting (OC) (Sartkulvanich, Koppka and Altan, 2004:61-71). Fu (2007:30) combined the SHPB and OC methods to determine the material parameters of Eq. 1. For Al7050-T7451, the physical properties and Johnson-Cook model parameters are shown in Table 1 and Table 2, respectively.

Table 1: Physical properties of workpiece (Al7050-T7451) and Tool material (YG6).

Physical parameter	Workpiece (Al7050-T7451)	Tool (YG6)
Density, ρ (kg/m3)	2800	14600
Elastic modulus, E (GPa)	69.35(20℃), 63(100℃), 57.09(200℃), 44.57(300℃)	630
Poisson's ratio, v	0.33	0.21
Specific heat, C_p (J/kg℃)	888(50℃), 904(100℃), 988(150℃), 1004(204℃), 1047(260℃)	400
Thermal conductivity, λ(W/m℃)	134(50℃), 142(100℃), 147(125℃), 176(200℃)	79.6
Linear Expansion coefficient, α (10^{-6}/℃)	23.6(100℃), 23.3(125℃), 23.5(150℃), 24(200℃)	-
T_{melt} (℃)	630℃	-
T_0 (℃)	25℃	-

Table 2: Johnson-Cook constitutive model parameters of Al 7050-T7451 (Fu, X.L., 2007).

A (MPa)	B (MPa)	C	n	m	$\dot{\varepsilon}_0$
463.4	319.5	0.027	0.32	0.99	1

2.2 ALE Chip Separation Approach

The ALE model is divided in several zones, and uses sliding, Lagrangian and Eulerian contours allowing the material to flow across an internal Eulerian zone surrounding the tool tip.

As shown in Figure 1, Zones 1, 2 and 3 combine Lagrangian/Eulerian boundaries with sliding boundaries, where the material is allowed to flow tangentially to the contour and not allowed to go across this boundary. At Eulerian zone 4, it is considered as a tube with one entrance and two exits, and the material enters on the left-hand

boundary and exits at the right-hand boundary and at the top surface. In order to retain the Eulerian boundaries, adaptive mesh constraints are endowed with both the X and Y direction of the zone 4.

The geometry of the baseline model with zero rake angle and cutting edge radius 0.02mm of tool, cutting depth 0.1mm and cutting width 1.5mm of workpiece is established. The tool is fixed and the cutting speed is applied to the workpiece. Continuous chip formation is assumed. The material flowed around the tool tip as if it is a fluid. In other words, there is no need to define a failure criterion.

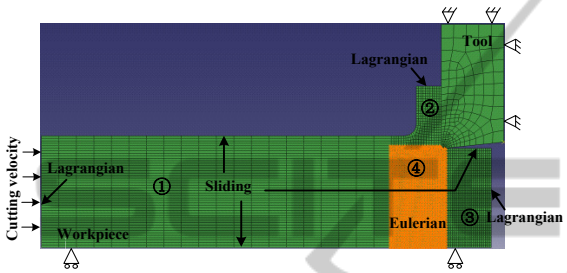

Figure 1: Illustration of ALE model.

2.3 PDZ Chip Separation Approach

Figure 2 illustrates the geometry of the orthogonal cutting model with a predefined cutting path, which is composed of four parts: (1) tool, (2) chip, (3) tool-tip passage zone and (4) workpiece. A chamfer is designed on part 2 to avoid distortion problems at the beginning of calculation. The centre of the tool tip is placed exactly at the middle height of part 3. The length and width of parallelogram mesh are set less than 20μm due to high shear localization.

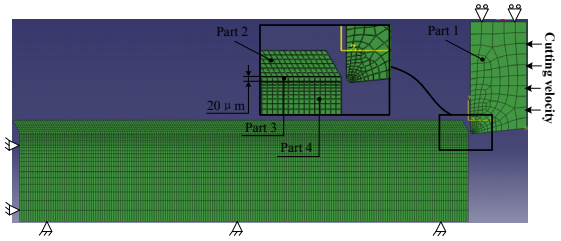

Figure 2: Illustration of ALE model.

The separation of the chip from the workpiece is based on a shear failure module which is applied to part 3. The shear failure module is based on the effective plastic strain $\bar{\varepsilon}$. When any element reaches the failure plastic strain value $\bar{\varepsilon}_f$, the damage parameter D, in Eq. 2 equals to one. When this occurs, the corresponding element will be deleted. The workpiece is fixed and the cutting speed is applied to the tool. Continuous chip formation is assumed. The tool geometry, cutting depth and cutting width of the workpiece is exactly the same as that used in ALE model.

$$D = \frac{\bar{\varepsilon}}{\bar{\varepsilon}_f} = 1 \tag{2}$$

2.4 Contact Modelling

The modified Coulomb friction model is adopted to describe the sliding and sticking phenomenon on the tool rake face. Figure 3 shows the characteristic of the model. Sticking or sliding friction conditions along the tool-chip interface are dependent on the shear stress magnitude. Sticking will occur at high contact pressure, as shown in the shaded region. When the contact pressure is low, as is the case away from the tool cutting edge, sliding friction will dominate (as shown in the unshaded region).

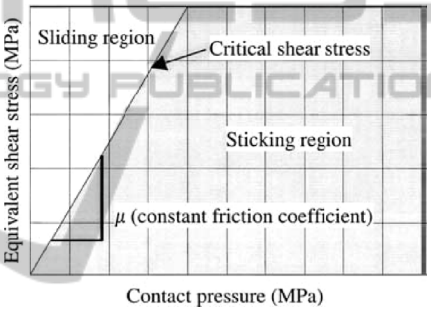

Figure 3: Stick-Slip region for the coulomb friction.

The following expression has been applied:

$$\tau = \mu p \quad \text{when } \mu p < \tau_{max} \text{ (sliding)} \tag{3}$$

$$\tau = \tau_{max} \quad \text{when } \mu p \geq \tau_{max} \text{ (sticking)} \tag{4}$$

where τ, p are the friction stress and the contact pressure on the tool rake face, respectively. τ_{max}, is the maximum shear stress of the material, and μ is the friction coefficient. In this study, the tendency of friction coefficient μ with cutting speed is obtained by the orthogonal cutting tests (Fu, 2007:50).

2.5 Heat Generation

Heat generation during metal cutting is important in tool wear and plays an important role in surface integrity and chip formation. The majority of the heat generated comes from plastic deformation and friction. The temperature increment associated with the heat generation are expressed by

$$\Delta T = \frac{f_1 f_2 \bar{\sigma} \cdot \partial \bar{\varepsilon}}{\rho C_p} \tag{5}$$

Where ΔT is temperature increment, f_1 is work-heat convection factor; f_2 is the conversion efficiency factor. f_1 and f_2 are taken as 0.9. $\partial\bar{\varepsilon}$ is the effective plastic strain increment. ρ and C_p are material density and specific heat. Heat transfer between tool and workpiece is not considered.

2.6 Analysis

Plane strain conditions are considered (as the workpiece width is at least ten times the chip thickness). An explicit resolution method with dynamic and coupled thermo-mechanical analysis is performed with CPE4RT element type.

Analysis is carried out in two steps. In the first step, cutting is modelled at constant cutting speed and steady state conditions are reached. In the second step, the workpiece is unloaded and cooled, and the residual stress profile is obtained.

3 RESULTS AND DISSCUSSION

3.1 Chip Formation

The comparison of the predicted chip and Mises stress at t=0.075ms and t=0.15ms for ALE and PDZ methods is shown in Figure 4. The chip curl of the PDZ method has larger radius than that of ALE method. Generally, the chip with a longer contact length with the tool produces a larger curl radius than that with a shorter contact. As the calculation time increases, the number of elements of ALE model in contact with the tool decreases because they are enlarged as well as the excessive distortion at the curvature zone of the chip, thus diminishing the accuracy of the calculation. Indeed, the chip from the PDZ model has twice longer contact length than that of ALE model. The chip curl is a key issue for the design of chip breakers, and good tool performance from the correct design.

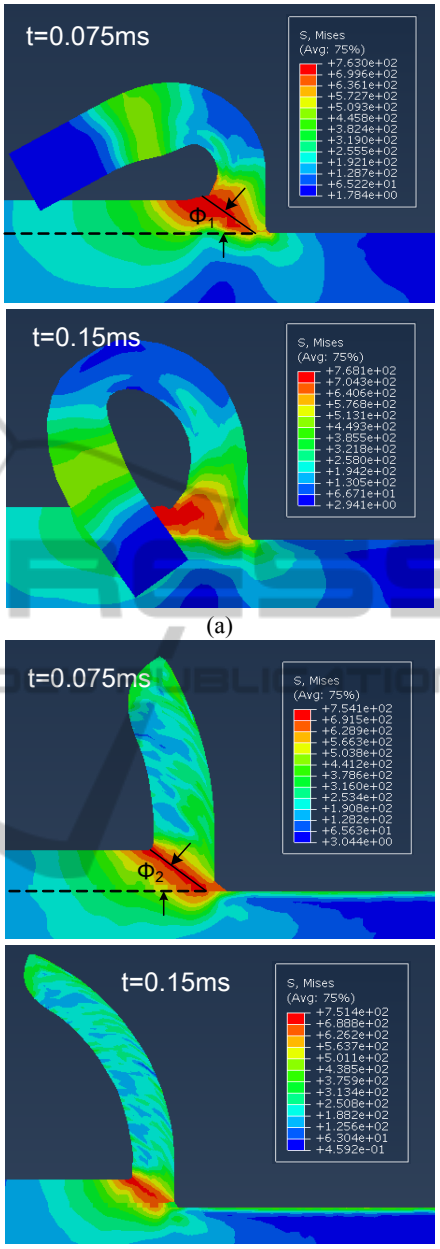

Figure 4: Chip formation process of (a) ALE, (b) PDZ method at v=800m/min.

3.2 Cutting Force

Figure 5 illustrates the predicted cutting force and feed force under different cutting speeds. It is clear that the predicted cutting force almost yield a similar pattern that the force magnitude decreases with the cutting speed. Small discrepancy is found between the predicted cutting force of the ALE and PDZ methods, which is less than 30N.

It is found that the predicted feed force of the ALE model is below that of PDZ model. Larger discrepancy between the predicted feed forces is found when the cutting speed over 800m/min. In PDZ model, the elements of the separation path are enlarged to failure which will apply an extra force perpendicular to the machined surface around the too-tip. As the cutting speed increases, the feed force is influenced significantly.

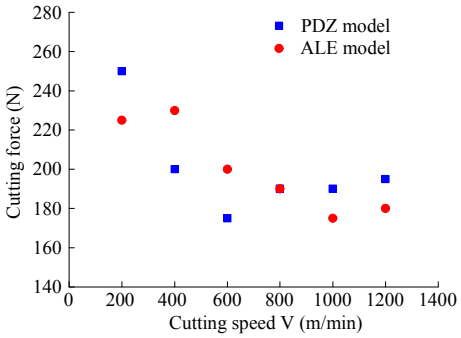

(a)

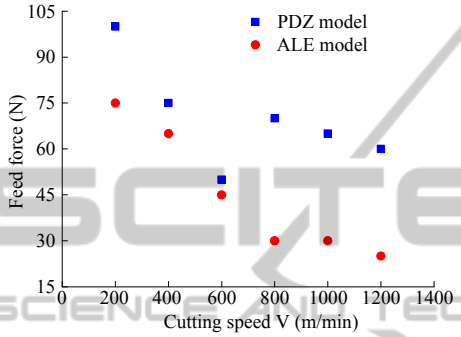

(b)

Figure 5: Predicted (a) cutting force and (b) feed force results under different cutting speeds.

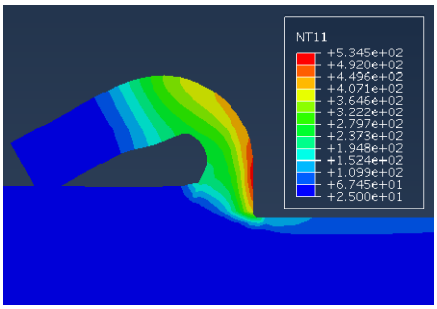

(a)

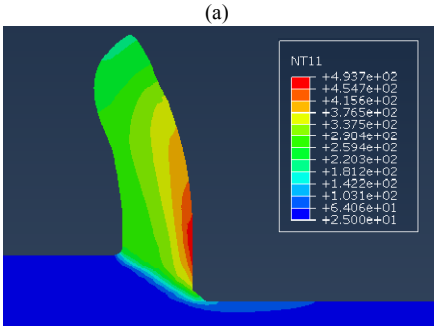

(b)

Figure 6: Predicted temperature distributions of (a) ALE, (b) PDZ, at v=800m/min.

3.3 Stress and Temperature Field

Figure 6 shows the instantaneous temperature fields at t=0.075ms. The predictions of ALE and PDZ model have a similar temperature distribution pattern. The highest temperature region occurs at the tool-chip interface, i.e., secondary shear zone. The maximum temperatures are 534.5°C and 493.7°C for ALE and PDZ model predictions, respectively, while the average temperature in the shear zone are 131.6°C and 122.6°C for the ALE and PDZ model.

In Figure 7, the stress distributions in the cutting direction S_{11} at t=0.075ms are depicted. In each case, the highest stress level is found in the first shear zone with the peak compressive stress in contact with the tool tip. The highest value of S_{11}, 1400MPa is found in the prediction using ALE method, while 1085MPa is found in the prediction using PDZ method. Moreover, strong stress fields exist in the zones in front of and behind the tool tip, in which compressive stress (green zone) dominates the front zone while tensile stress dominates the back zone (red zone) due to the effect of tool flank.

However, the stress distribution patterns on the produced new surface are quite different for ALE and PDZ methods, which are tensile stress dominated and compressive stress dominated respectively.

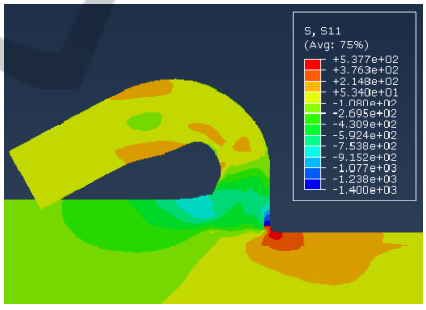

(a)

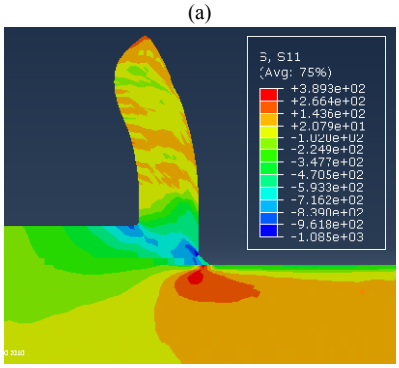

(b)

Figure 7: Predicted S_{11} distributions of (a) ALE, (b) PDZ, at v=800m/min.

3.4 Residual Stress

The effect of chip separation and cutting speeds on

the predicted residual stresses in cutting direction (RS_{11}) is shown in Figure 8.

For each cutting speed, ALE method produces tensile stress on the surface, and the magnitude of RS11 decreases within the depth of 100 μm below the machined surface. Then, the RS_{11} tends to be constant as the depth over 100μm. This pattern agrees well with the computed residual stress results of Nasr (2008:149-161) using ALE method, which are also verified by the experiments. On the other hand, PDZ method produces compressive stress on the surface, and the RS_{11} increases within depth of 100 μm below the machined surface. Then, the RS_{11} tends to be constant as the depth over 100μm.

The effect of cutting speeds on the predicted RS_{11} is also different for ALE and PDZ methods. The predicted peak magnitude of RS_{11} by ALE method decreases as the cutting speed increases, which is generally reported in literature. On the other hand, the predicted peak magnitude of RS_{11} by PDZ method increases proportionally as the cutting speed increases.

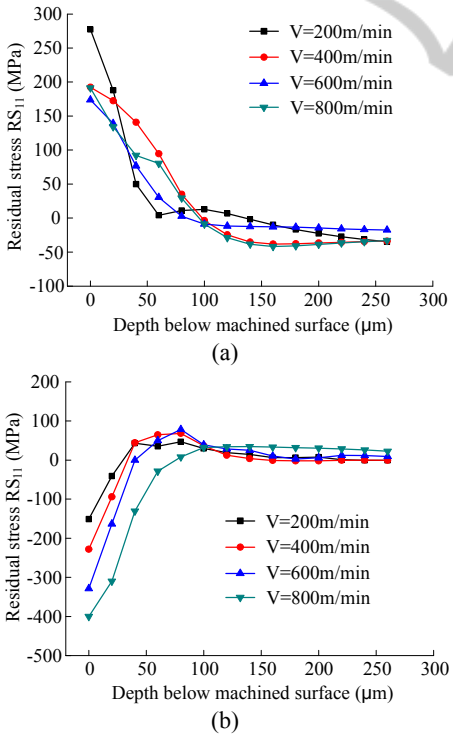

Figure 8: Predicted residual stress profiles of (a) ALE, (b) PDZ method under different cutting speeds.

The primary cause of residual stress generation is plastic deformation. In order to explain the different residual stress predictions, the plastic strain in the cutting direction (PE11) of the machined surface around the tool-tip are shown in Figure 9. It is clear that ALE method produces the compressive strain on the surface and near-surface layers, with the peak value of 0.06. But PDZ method produces the tensile strain with the peak value of 0.01. After the workpiece is unloaded and cooled, the residual stress will becomes tensile and compressive dominated, respectively.

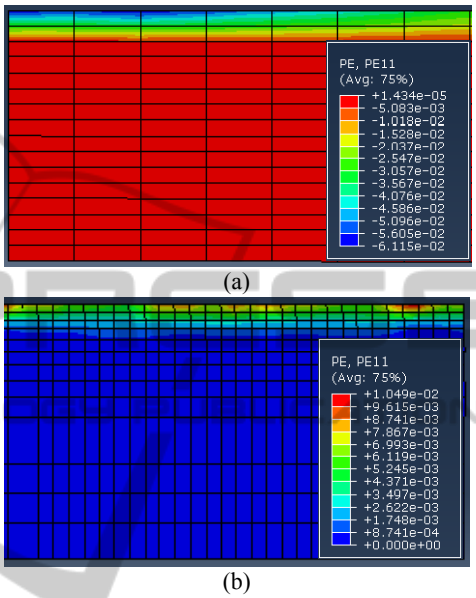

Figure 9: Predicted strain distributions of (a) ALE, (b) PDZ method, at v=800m/min.

The combination of mechanical and thermal loading produces the strain results, and it is noticed the cutting force and temperature predictions are similar for ALE and PDZ methods. It is interesting that the same thermo-mechanical loading produces different strain results.

It is noticed that the elements of the separation path in PDZ model are enlarged to failure which will drag the element on the new produced surface. As a result, the tensile dominated strain state is formed. On the other hand, ALE method handles the material flow surrounding the tool-tip perfectly, thus the material exiting at the right-hand boundary of Eulerian zone is merely affected by the tool flank. As a result, the compressive dominated strain state is formed in the prediction of ALE model.

4 CONCLUSIONS

Based on the prediction results and discussions, the following conclusions are obtained:

- Chip formation predicted by ALE and PDZ methods is quite different. ALE method is difficult to predict reasonable chip formation.
- ALE and PDZ methods predict similar cutting force and temperature predictions.
- ALE and PDZ methods predict different residual stress profiles, and the possible reasons are discussed through the strain results around the tool-tip.

ACKNOWLEDGEMENTS

The authors acknowledge the support from the National Basic Research Program of China (No.2010CB731703) and National Natural Science Foundation of China (No.51075267).

REFERENCES

Shet, C., Deng, X., 2003. 'Residual stress and strain in othogonal metal cutting', *Int. J. Mach. Tool. Manu*, vol. 43, pp. 573-583.

Hortig, C., Svendsen, B., 2007. 'Simulation of chip formation during high-speed cutting', *J. Mater. Process. Tech*, vol. 186, pp. 66-76.

Ng, E-G., El-Wardany, T-I., Dumitrescua, M., and Elbestawia, M. A., 2002. 'physics-based simulation of high speed machining', *Mach. Sci. Technol*, vol. 6, no. 3, pp. 301-329.

Mabrouki, T., Girardin, F., Asad, M., and Rigal, J-F., 2008. 'Numerical and experimental study of dry cutting for an aeronautic aluminium alloy (A2024-T351)', *Int. J. Mach. Tool. Manu*, vol. 48, pp. 1187-1197.

Pantalé, O., Bacaria, J-L., Dalverny, O., Rakotomalala, R., and Caperaa, S., 2004. '2D and 3D numerical models of metal cutting with damage effects', *Comput. Methods Appl. Mech. Engrg*, vol. 193, pp.4383-4399.

Anurag, S., Guo, Y.B., and Horstemeyer, M.F., 2009. 'The effect of materials testing modes on finite element simulation of hard machining via the use of internal state variable plasticity model coupled with experimental study', *Comput. Struct*, vol. 87, pp. 303-317.

Nasr, M.N.A., Ng, E-G., and Elbestawi, M.A., 2007. 'Modelling the effects of tool-edge radius on residual stresses when orthogonal cutting AISI 316L', *Int. J. Mach. Tool. Manu*, vol. 47, pp.401-411.

Movahhedy, M.R., Gadala, M.S., and Altintas, Y., 2000. 'Simulation of the orthogonal metal cutting process using an arbitrary Lagrangian-Eulerian Finite element method', *J. Mater. Process. Tech*, vol. 103. pp.267-275.

Kim, K.W., Lee, W.Y., and Sin, H.C., 1999. 'A finite-element analysis of machining with the tool edge considered', *J. Mater. Process. Tech*, vol. 86, pp.45-55.

Strenkowski, J.S., Shih, A.J., and Lin, J-C., 2002. 'An analytical finite element model for predicting three-dimensional tool forces and chip flow', *Int. J. Mach. Tool. Manu*, vol. 42, no. 6, pp.723-731.

Nasr, M.N.A., Ng, E-G., and Elbestawi, M.A., 2008. 'A modified time-efficient FE approach for predicting machining-induced residual stresses', *Finite. Elem. Anal. Des*, vol. 44, pp.149-161.

Lennon, A.M. and Ramesh, K.T., 1998. 'A technique for measuring the dynamic behaviour of materials at high temperatures', *Int. J. Plasticity*, vol. 14, pp.1279-1292.

Sartkulvanich, P., Koppka, F., and Altan, T., 2004. 'Determination of flow stress for metal cutting simulation-a progress report', *J. Mater. Process. Tech*, vol. 146, pp.61-71.

Fu, X.L., 2007. 'Research on deformation theory and characteristics of machined surface for high-speed milling aviation aluminium alloy', Ph.D dissertation, Shandong university, JiNan.